VERSITA

GEOCHRONOMETRIA 40(4) 2013: 244-249
DOI 10.2478/s13386-013-0130-9

Available online at
www.springerlink.com

RESPONSE OF CATHODOLUMINESCENCE OF ALKALI FELDSPAR TO He^+ ION IMPLANTATION AND ELECTRON IRRADIATION

MASAHIRO KAYAMA[1], HIROTSUGU NISHIDO[2], SHIN TOYODA[3], KOSEI KOMURO[4], ADRIAN A. FINCH[5], MARTIN R. LEE[6] and KIYOTAKA NINAGAWA[3]

[1]*Department of Earth and Planetary Systems Science, Graduate School of Science, Hiroshima University, 1-3-1 Kagami-yama, Higashi-Hiroshima, Hiroshima 739-8526, Japan*
[2]*Department of Biosphere-Geosphere Science, Okayama University of Science, 1-1 Ridaicho, Kita-ku, Okayama, Okayama 700-0005, Japan*
[3]*Department of Applied Physics, Okayama University of Science, 1-1 Ridaicho, Kita-ku, Okayama, Okayama 700-0005, Japan*
[4]*Earth Evolution Sciences, University of Tsukuba, 1-1-1 Ten-nodai, Tsukuba, Ibaraki, 305-8571, Japan*
[5]*Department of Earth Sciences, University of St Andrews, Irvine Building, North Street, St Andrews, Fife, KY16 9AL, UK*
[6]*School of Geographical and Earth Sciences, University of Glasgow, Lilybank Gardens, Glasgow G12 8QQ, UK*

Received 29 January 2013 Accepted 27 August 2013

Abstract: Cathodoluminescence (CL) of minerals such as quartz and zircon has been extensively studied to be used as an indicator for geodosimetry and geochronometry. There are, however, very few investigations on CL of other rock-forming minerals such as feldspars, regardless of their great scientific interest. This study has sought to clarify the effect of He^+ ion implantation and electron irradiation on luminescent emissions by acquiring CL spectra from various types of feldspars including anorthoclase, amazonite and adularia. CL intensities of UV and blue emissions, assigned to Pb^{2+} and Ti^{4+} impurity centers respectively, decrease with an increase in radiation dose of He^+ ion implantation and electron irradiation time. This may be due to decrease in the luminescence efficiencies by a change of the activation energy or a conversion of the emission center to a non-luminescent center due to an alteration of the energy state. Also, CL spectroscopy of the alkali feldspar revealed an increase in the blue and yellow emission intensity assigned to Al-O^--Al/Ti defect and radiation-induced defect centers with the radiation dose and the electron irradiation time. Taken together these results indicate that CL signal should be used for estimation of the α and β radiation doses from natural radionuclides that alkali feldspars have experienced.

Keywords: cathodoluminescence, alkali feldspar, He^+ ion implantation, electron irradiation.

1. INTRODUCTION

Dose of natural radiation, especially γ ray that have been accumulated by rock-forming minerals such as feldspar and quartz has been quantitatively estimated using thermoluminescence (TL), optically stimulated luminescence (OSL) and electron spin resonance (ESR) analyses for determining the geological age of sedimentary rocks and volcanic ejecta, tracking the transportation and deposition of fluvial sediments and determining provenance (Wintle and Huntley, 1979; Guerin and Valldas, 1980; Huntley *et al.*, 1985; Petrov, 1994; Shirai *et al.*, 2008). These techniques allow us to determine the density of various types of lattice defects produced by

Corresponding author: M. Kayama
e-mail: kayama27@hiroshima-u.ac.jp

ISSN 1897-1695 (online), 1733-8387 (print)

natural radiation over geological timescale. Recent scientific interest in radiation effects on minerals focus not only on such geological applications, but also geoscientific and planetary scientific applications, e.g., observation of pleochroic halo in quartz and feldspar generated by natural radiation from the disintegration of radioactive elements (Nasdala *et al.*, 2006), clarification of release process of Na atoms from plagioclase on the surface of the Moon and Mercury into the exospheres due to space weathering (Sprague *et al.*, 2002; Wurz and Lammer, 2003; Lowitzer *et al.*, 2008) and detection of food irradiation (Soika and Delincée, 2000). These radiation effects on minerals, caused mainly by ions, protons and electrons as well as α particles, are seen from the grain surface to a depth of several tens to hundreds of micrometers. For this reason, they have not been clarified in detail because the conventional analytical methods require the extraction of large quantities of the mineral grains from the target rocks.

Cathodoluminescence (CL) is the emission of photons of ultraviolet (UV) to infrared (IR) wavelengths from a material stimulated by an incident electron beam, and is an important tool for characterization of radiation damage on minerals that coexisted with natural radionuclides (e.g., quartz with zircon and feldspar with euxenite). CL spectroscopy and microscopy provide valuable information on the existence and distribution of defects and trace elements in minerals with a spatial resolution of a few micrometers. According to Stevens-Kalceff *et al.* (2000) and King *et al.* (2011), He^+ ion implantation and electron irradiation significantly affect the CL properties of minerals as change of CL is activated by impurity and radiation-induced defect centers. CL analysis allow us to estimate their radiation effects on the mineral grains with high spatial resolution. Recently, CL measurements on ion-implanted and electron irradiated quartz and albite have enabled interpretation of radiation effects, including observation of micrometer-sized radiation halos produced by α particles and estimation of the α and β radiation doses as geodosimetry (Owen, 1988; Komuro *et al.*, 2002; Okumura *et al.*, 2008; Krickl *et al.*, 2008; Kayama *et al.*, 2011a; Kayama *et al.*, 2011b; King *et al.*, 2011). Although great scientific interest exists concerning CL of radiation-induced quartz and albite, very few such investigations have been carried out for alkali feldspars up to now.

In this study, He^+ ion implantation experiment was conducted using a 3M-tandem ion accelerator at 4.0 MeV, corresponding to the energy of α particles generated by the disintegration of ^{238}U and ^{232}Th, and electron irradiation experiment was performed for various types of alkali feldspars. Also, this study has sought to determine their impact of radiations on alkali feldspars and to apply for geodosimetry and geochronometry.

2. SAMPLES AND METHODS

CL microscopy and spectroscopy were carried out for single crystals of anorthoclase (Ano) from Kobushi, Nagano, Japan, amazonite (Ama) from Rio Doce, Minas Gerais, Brazil and adularia (Adu) from Ritleskopf, Rauris, Austria. Slices of the single crystals (10 × 10 × 1 mm) were polished and finished with a 1 μm diamond abrasive.

The He^+ ion implantation experiment was performed perpendicularly to the surfaces of the slices using a 3M-tandem ion accelerator located at Takasaki Research Center of the Japan Atomic Energy Research Institute. The ion-beam had a 4.0 MeV implantation energy which corresponds to the energy of an α particle from ^{238}U and ^{232}Th disintegrations. A specific dose density was set in the range from 6.38×10^{-6} to 5.10×10^{-4} C/cm^2 for anorthoclase, 7.36×10^{-6} to 4.83×10^{-4} C/cm^2 for amazonite and 2.18×10^{-6} to 6.33×10^{-4} C/cm^2 for the adularia. The implanted samples are denoted according to their dose density, e.g., Ano00 for unimplanted anorthoclase and Ano08 for anorthoclase that received the highest dose. CL spectra were acquired from the implanted surface of the samples, which are labelled "S" after each sample number, e.g., Ama01S for the implanted amazonite at lowest dose and Ama08S for amazonite at highest dose. Furthermore, the implanted samples were cut perpendicularly to the exposed surfaces for high-resolution CL imaging of the cross-section. The cross section is denoted by "C" after the sample identifier, e.g., Adu00C for unimplanted adularia and Adu10C for the implanted adularia at highest radiation dose. The details of the He^+ ion implantation experiments and sample preparation are described by Okumura *et al.* (2008) and Kayama *et al.* (2011a).

Prolonged electron irradiation experiments were conducted on unimplanted and He^+-ion-implanted alkali feldspars at the highest radiation doses. The electron irradiation was undertaken in a scanning electron microscopy-cathodoluminescence (SEM-CL), composed of SEM (JEOL: JSM-5410) and a grating monochromator (Oxford: Mono CL2), operated at a 15 kV accelerating voltage and 50 nA beam current. The electron beam was scanned over an area of 110 × 93 μm for 600 s.

SEM-CL analysis was also used to obtain CL spectra with operating conditions of 15 kV and 2.0 nA in scanning mode with a 110 × 93 μm scanning area. All CL spectra were obtained in the range from 300 to 800 nm in 1 mm steps and were corrected for the total instrumental response using a calibrated standard lamp. High-resolution CL images were observed using a Gatan: MiniCL imaging system under the same conditions as CL spectral analysis using SEM-CL. More details of the equipment construction and analytical procedures can be found in Ikenaga *et al.* (2000) and Kayama *et al.* (2010).

3. RESULTS AND DISCUSSION

Panchromatic CL images of the cross-sections of the implanted adularia (Adu01C to Adu10C) consist of a bright luminescent band on the dull luminescent background, but those of the anorthoclase (Ano01C to Ano08C) and amazonite (Ama01C to Ama08C) show a ~1 μm thick dark line with width of a few micrometers on a bright luminescent background at 12 to 15 μm beneath the implanted surface (**Fig. 1**). The bright luminescent band and dark line are identified as CL halo from the He^+-ion-implanted surface. With an increase in radiation dose of He^+ ion implantation, intensities of the CL halos tend to increase for adularia, but decrease for anorthoclase and amazonite. These facts imply that He^+ ion implantation causes a drastic change in CL properties of adularia, anorthoclase and amazonite, but the behavior varies between alkali feldspars. The distance of the CL halos from the implanted surface is consistent with the maximum of electronic energy loss of 4.0 MeV He^+ ion in alkali feldspars (Bragg and Kleeman, 1905; Nogami and Hurley, 1948; Faul, 1954; Owen, 1988; Komuro *et al.*, 2002; Okumura *et al.*, 2008). CL line analysis, acquired through the cross-sections of the implanted alkali feldspars from the implanted surface to a depth of 20 μm including the CL halo at 12 to 15 μm, shows exponential increase for the adularia and decreases for the anorthoclase and amazonite in intensities along the depth direction down to 15 μm, and exhibits subsequently decrease and increase over this point, respectively. The increasing and decreasing behavior corresponds to the energy loss process of charge particles (Bragg and Kleeman, 1905; Nogami and Hurley, 1948; Faul, 1954; Owen, 1988; Komuro *et al.*, 2002; Okumura *et al.*, 2008; Kayama *et al.*, 2011a). A similar phenomenon has been recognized in previous CL studies on He^+-ion-implanted albite, sanidine, orthoclase and microcline (Kayama *et al.*, 2011a; Kayama *et al.* in submitted); He^+ ion implantation on these feldspars leads to a formation of CL halo with width corresponding to the energy loss of 4.0 MeV He^+ ions and results in decreasing and increasing of their CL with radiation dose, which are responsible for a change in luminescence efficiency, a conversion of the emission center into non-luminescent center, a trap of electron holes at the lattice defect and formation of radiation-induced defect center. These processes caused by He^+ ion implantation may also contribute to the observed changes of CL in the adularia, anorthoclase and amazonite.

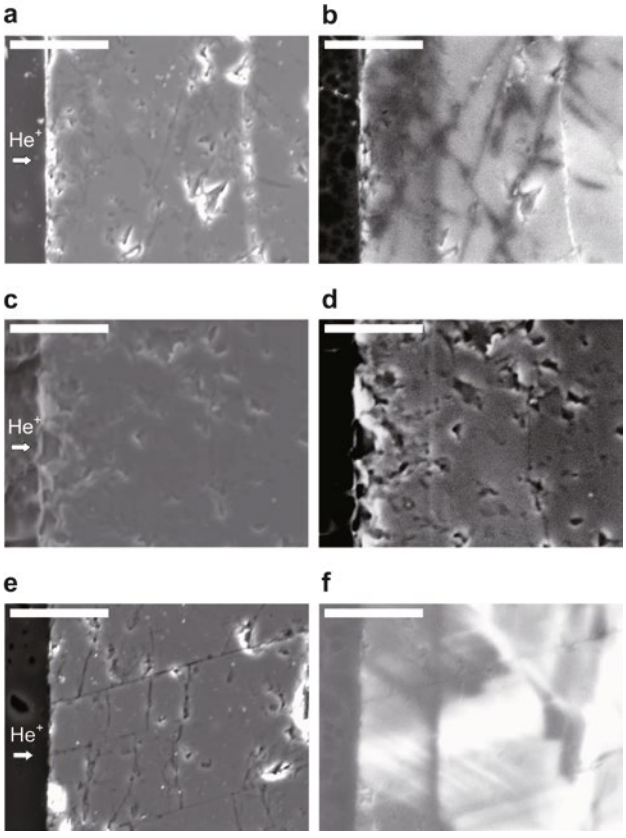

Fig. 1. *Secondary electron and panchromatic CL images of cross-sections of He^+-ion-implanted (a), (b) anorthoclase, (c), (d) adularia and (e), (f) amazonite, respectively. Scale bars are 20 μm.*

CL spectra of unimplanted, He^+-ion-implanted and electron irradiated anorthoclase, amazonite and adularia consist of emission bands centered below 300 nm, peaking at ~320, ~350, ~420, ~440, ~580 and 700-750 nm (**Figs. 2**, **3** and **4**). Their luminescence properties such as intensity, peak wavelength and shape vary with radiation dose of the He^+ ion implantation and electron irradiation time, of which the impact differs between emission bands, as well as alkali feldspars. The UV emissions below 300 nm is observed in CL spectra of unimplanted, He^+-ion-implanted and electron irradiated amazonite and adularia (**Figs. 3** and **4**), and may be corresponding to the emission band at 284 nm assigned to the Pb^{2+} impurity center (Vaggelli *et al.*, 2005). Unimplanted, He^+-ion-implanted and electron irradiated anorthoclase and adularia have an emission band at ~420 nm in blue region (**Figs. 2** and **4**), which is activated by Ti^{4+} impurity centers (Mariano *et al.*, 1973; Finch and Klein, 1999; Götze *et al.*, 2000; Lee *et al.*, 2007; Parsons *et al.*, 2008; Kayama *et al.*, 2010). CL intensities of these UV and blue emissions decrease with increases in radiation dose of He^+ ion implantation and electron irradiation time. Previous studies of He^+-ion-implanted and electron irradiated plagioclase revealed a similar decrease in the CL intensity depending on the radiation dose and the irradiation time, which may be closely related to partial destruction of the feldspar framework and migration of Na^+ cations judging from Raman spectroscopy and chemical analysis by wavelength dispersive X-ray spectroscopy (Kayama *et al.*, 2011a, 2013). Therefore, He^+ ion implantation may destroy the atomic bonds between impurity centers such as Pb^{2+} and Ti^{4+} and their ligands in the present alkali feldspars, and electron irradiation may migrate Na^+ cations located near the impurity centers, leading to a de-

crease in the luminescence efficiencies by a change of the activation energy or a conversion of the emission center to a non-luminescent center due to an alteration of the energy state. These may be responsible for a reduction of the UV and blue CL intensity caused by Pb^{2+} and Ti^{4+} impurity centers.

Unimplanted, He^{+}-ion-implanted and electron irradiated amazonite have blue CL emissions at ~440 nm (**Fig. 3**). According to Kayama *et al.* (2010), the emission band in blue spectral region consists of an overlap of two emission components, namely the oxygen defect centers associated with Al-O-Al and Al-O-Ti bridges (Al-O^{-}-Al/Ti defect center) and the Ti^{4+} impurity center. The component assigned to Al-O^{-}-Al/Ti defect center is located at longer peak wavelength (2.815-2.845 eV) than that to Ti^{4+} impurity centers (3.055-3.076 eV). It implies that Al-O^{-}-Al/Ti defect center acts as a dominant activator for the emission bands at ~440 nm in the present amazonite, rather than Ti^{4+} impurity center. The emission band at ~440 nm in amazonite shows an increase in the intensities with radiation dose of He^{+} ion implantation and electron irradiation time (**Fig. 3**). King *et al.* (2011) demonstrated that ion implantation on quartz changes the $[AlO_4/M^{+}]^0$ defect (M: H^{+}, Li^{+}, Na^{+} and K^{+}) into the $[AlO_4]^0$ defect due to trapping of electron holes derived from the Na^{+} migration at the latter defect, leading to an increase in the blue emission intensity with elevated radiation doses. The Al-O^{-}-Al/Ti defect center in feldspar is composed of electron hole trapped at Löwenstein bridges and therefore produced by Na^{+} migration during ion implantation as well as electron irradiation (Kayama *et al.* in submitted). Also, an enhancement of the blue CL in the amazonite may be caused by formation of Al-O^{-}-Al/Ti defect centers due to the Na^{+} migration and trap accompanying He^{+} ion implantation and electron irradiation.

The red-IR emissions at 700-750 nm are also detectable in CL spectra of unimplanted, He^{+}-ion-implanted and electron irradiated anorthoclase and amazonite (**Figs. 2** and **3**), and are attributed to a Fe^{3+} impurity that substitutes for Al^{3+} ions in tetrahedral sites for the luminescence caused by the radiative transition of the electrons from $^4T_1$ to $^6A_1$ (Telfer and Walker, 1978; Finch and Klein, 1999; Götze *et al.*, 2000). According to Finch and Klein (1999) and Kayama *et al.* (2010), two components assigned to Fe^{3+} impurity centers on T1 and T2 sites constitute the red-IR CL emission. There is an increase in the red-IR emission intensities of the anorthoclase and amazonite with enhanced radiation dose of He^{+} ion implantation and electron irradiation time. Furthermore, the peak position of the red-IR emission band in anorthoclase shifts to a longer-wavelength side with radiation dose of He^{+} ion implantation. Such increasing and peak shift of the red-IR CL may be due to an energy transition between Fe^{3+} impurity centers on T1 and T2 sites. According to Kayama *et al.* (in submitted), a partial destruction of the feldspar frameworks and the Na^{+} migration due to He^{+} ion implantation and electron irradiation reduce the

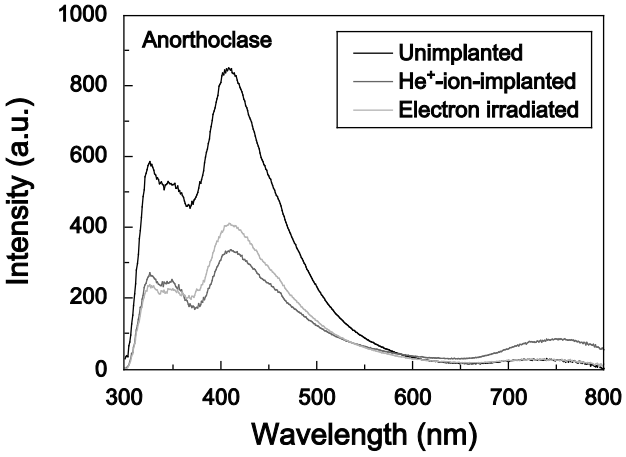

Fig. 2. *CL spectra of anorthoclase (a) unimplanted, (b) He^{+}-ion-implanted anorthoclase at 5.10 × 10^{-4} C/cm² (Ano08S) and (c) electron irradiated at 50 nA for 600 s.*

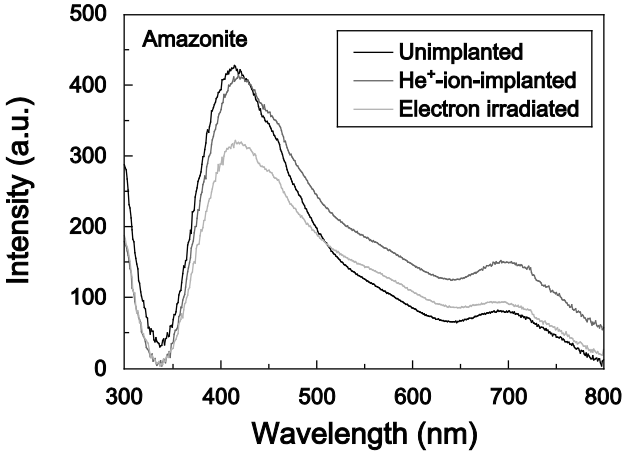

Fig. 3. *CL spectra of amazonite (a) unimplanted, (b) He^{+}-ion-implanted at 4.83 × 10^{-4} C/cm² (Ama08S) and (c) electron irradiated at 50 nA for 600 s.*

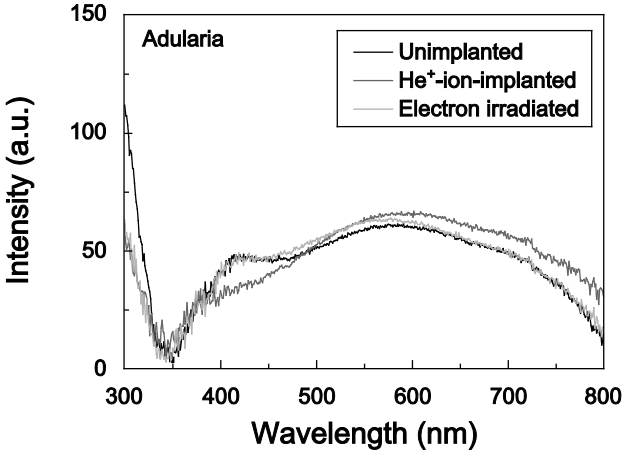

Fig. 4. *CL spectra of adularia (a) unimplanted, (b) He^{+}-ion-implanted at 6.33 × 10^{-4} C/cm² (Adu10S) and (c) electron irradiated at 50 nA for 600 s.*

luminescence efficiency of Fe^{3+} impurity center on T1 site as a consequence of a change of activation energy or a conversion of the emission center into non-luminescent center by an alteration of the energy state, the same as in the case of Pb^{2+} and Ti^{4+} impurity center. Therefore, much of the energy for CL from the Fe^{3+} impurity center on the T1 site should be dissipated by radiative transition of Fe^{3+} impurity center on T2 site as the energy transition process, which may contributes to the enhancement and peak shift of the red-IR CL in anorthoclase and amazonite.

The emission band at ~580 nm occurs in CL spectrum of He^+-ion-implanted anorthoclase, but it is absent from that of unimplanted anorthoclase (**Fig. 2**). CL spectra of the amazonite and adularia also have similar yellow emissions at ~580 nm and reveal an increase in yellow emission intensities with radiation dose of He^+ ion implantation and electron irradiation time (**Figs. 3** and **4**). Kayama *et al.* (2011a, 2011b) demonstrated that He^+-ion-implanted albite show a comparable increase in the CL intensity depending on the radiation dose, which is characteristic of the radiation-induced defect center. He^+ ion implantation and electron irradiation, therefore, lead to a formation of the radiation-induced defect center, resulting in an increase of yellow CL of the present alkali feldspar. The rate of increase of the yellow emission intensity, however, differs significantly between alkali feldspar samples with comparable radiation doses of He^+ ion implantation and electron irradiation time, which may be closely related to the degree of Si-Al ordering and chemical composition. As the intensities of the yellow emission assigned to the radiation-induced defect center and the blue emission to the Al-O^--Al/Ti defect centers increase with radiation dose of He^+ ion implantation and electron irradiation time, these CL signals have great potential for estimation of the natural α and β radiation doses that micro-ordered alkali feldspar has experienced, based on the correction of CL spectral data for the degree of the Si-Al ordering and chemical composition.

ACKNOWLEDGMENTS

We are deeply indebted to S. Nakano for helpful suggestions on CL of feldspar. He^+ ion implantation experiments were supported by the Inter-University Program for the Joint Use of the Japan Atomic Energy Agency (Takasaki), grant No. 12010 to H. N.

REFERENCES

Bragg WH and Kleeman R, 1905. Alpha particles or radium, and their loss of range passing through various atoms and molecules. *Philosophical Magazine* 10: 318-334.

Faul H, 1954. *Nuclear Geology*. John Wiley, New York, 414.

Finch AA and Klein J, 1999. The causes and petrological significance of cathodoluminescence emission from alkali feldspars. *Contributions to Mineralogy and Petrology* 135: 234-243.

Guerin G and Valldas G, 1980. Thermoluminescence dating of volcanic plagioclase. *Nature* 286: 697-699, DOI 10.1038/286697a0.

Götze J, Krbetschek MR, Habermann D and Wold D, 2000. High-resolution cathodoluminescence of feldspar minerals. In: Pagel M, Barbin V, Blanc P and Ohnenstetter D, eds., *Cathodoluminescence Geosciences*. Springer Verlag, Berlin, 245-270.

Huntley DJ, Godfrey-Smith DI and Thewalt MLW, 1985. Optical dating of sediments. *Nature* 313: 105-107, DOI 10.1038/313105a0.

Ikenaga M, Nishido H and Ninagawa K, 2000. Performance and analytical conditions of cathodoluminescence scanning electron microscope (CL-SEM). *The Bulletin of Research Institute of Natural Sciences Okayama University of Science.* 26: 61-75.

Kayama M, Nakano S and Nishido H, 2010. Characteristics of emission centers in alkali feldspar: A new approach by using cathodoluminescence spectral deconvolution. *American Mineralogist* 95: 1783-1795.

Kayama M, Nishido H, Toyoda S, Komuro K, Finch AA, Lee MR and Ninagawa K, in submitted. Cathodoluminescence properties of radiation-induced alkali feldspars. *American Mineralogist*.

Kayama M, Nishido H, Toyoda S, Komuro K and Ninagawa K, 2011a. Radiation effects on cathodoluminescence of albite. *American Mineralogist* 96: 1238-1247.

Kayama M, Nishido H, Toyoda S, Komuro K and Ninagawa K, 2011b. Combined Cathodoluminescence and Micro-Raman Study of Helium-Ion-Implanted Albite. *Spectroscopy Letters.* 44: 526-529.

Kayama M, Nishido H, Toyoda S, Komuro K, Finch AA, Lee MR and Ninagawa K, 2013. He^+ ion implantation and electron irradiation effects on cathodoluminescence of plagioclase. *Physics and Chemistry of Minerals* 40(7): 531-545, DOI 10.1007/s00269-013-0590-8.

King GE, Finch AA, Robinson RAJ and Hole DE, 2011. The problem of dating quartz 1: Spectroscopic ionoluminescence of dose dependence. *Radiation Measurements* 46(1): 1-9, DOI 10.1016/j.radmeas.2010.07.031.

Komuro K, Horikawa Y and Toyoda S, 2002. Development of radiation-damage halos in low-quartz: cathodoluminescence measurement after He^+ ion implantation. *Mineralogy and Petrology* 76(3-4): 261-266, DOI 10.1007/s007100200045.

Krickl R, Nasdala L, Götze J, Grambole D and Wirth R, 2008. Alpha-irradiation effects in SiO_2. *European Journal of Mineralogy.* 20: 517-522, DOI 10.1127/0935-1221/2008/0020-1842.

Lee MR, Parsons I, Edwards PR and Martin RW, 2007. Identification of cathodoluminescence activators in zoned alkali feldspars by hyperspectral imaging and electron-probe microanalysis. *American Mineralogist* 92: 243-253.

Lowitzer S, Wilson DJ, Winkler B, Milman V and Gale JD, 2008. Defect properties of albite: A combined empirical potential and density functional theory study. *Physics and Chemistry of Minerals* 35(3): 129-135, DOI 10.1007/s00269-007-0204-4.

Mariano AN, Ito J and Ring PJ, 1973. Cathodoluminescence of plagioclase feldspars. *Geological Society of America, Abstract Program* 5: 726.

Nasdala L, Wildner M, Wirth R, Groschopf N, Pal DC and Möller A, 2006. Alpha particle haloes in chlorite and cordierite. *Mineralogy and Petrology* 86(1-2): 1-27, DOI 10.1007/s00710-005-0104-6.

Nogami H and Hurley PM, 1948. The absorption factor in counting alpha rays from thick mineral sources. *American Geophysical Union Transactions*. 29: 335-340.

Okumura T, Nishido H, Toyoda S, Kaneko T, Kosugi S and Sawada Y, 2008. Evaluation of radiation-damage halos in quartz by cathodoluminescence as a geochronological tool. *Quaternary Geochronology* 3(4): 342-345, DOI 10.1016/j.quageo.2008.01.006.

Owen MR, 1988. Radiation-damage halos in quartz. *Geology* 16: 529-532, DOI 10.1130/0091-7613(1988)016<0529:RDHIQ>2.3.CO;2.

Parsons I, Steele DA, Lee MR and Magee CW, 2008. Titanium as a cathodoluminescence activator in alkali feldspar. *American Mineralogist* 93: 875-879.

Petrov I, 1994. Lattice-stabilized CH_3, C_2H_3, NO_2, and O^{1-} radicals in feldspar with different Al-Si order. *American Mineralogist* 79: 221-239.

Shirai M, Tsukamoto S and Kondo R, 2008. Transport-depositional processes of present fluvial deposits estimated from OSL intensity

of sand-size grains. *Quaternary Research* 47(3): 337-389, DOI 10.1006/qres.1997.1894.

Soika C and Delincée H, 2000. Thermoluminescence analysis for detection of irradiated food- effects of dose rate on the glow curves of quartz. *Lebensmittel-Wissensvhaft & Technologie*. 33: 440.

Sprague AL, Emery JP, Donldson KL, Russel RW, Lynch DK and Mazuk AL, 2002. Mercury: mid infrared (3-13 μm) observations show heterogeneous composition, presence of intermediate and basic soil types, and pyroxene. *Meteoritics and Planetary Science* 37(9): 1255-1268, DOI 10.1111/j.1945-5100.2002.tb00894.x.

Stevens-Kalceff MA, Matthew RP, Anthony RM and Kalceff W, 2000. Cathodoluminescence microcharacterisation of silicon dioxide polymorphs. In: Pagel M, Barbin V, Blanc P and Ohnenstetter D, eds., *Cathodoluminescence in Geosciences*. Springer, Berlin, 8: 193-223.

Telfer DJ and Walker G, 1978. Ligand field bands of Mn^{2+} and Fe^{3+} luminescence centers and their site occupancy in plagioclase feldspar. *Modern Geology* 6: 199-210.

Vaggelli G, Borghi A, Cossio R, Fedi M, Fiora L, Giuntini L, Massi M and Olmi F, 2005. Combined micro-PIXE facility and monochromatic cathodoluminescence spectroscopy to coloured minerals of natural stones: an example from amazonite. *X-ray spectrometry* 34: 345-349.

Wintle AG and Huntly DJ, 1979. Thermoluminescence dating of a deep-sea sediment core. *Nature* 279: 710-712, DOI 10.1038/279710a0.

Wurz P and Lammer H, 2003. Monte-Carlo simulation of Mercury's exosphere. *Icarus* 164(1): 1-13, DOI 10.1016/S0019-1035(03)00123-4.